

# CARACTERIZAÇÃO ESTRUTURAL DO ÁCIDO 2-AMINO-2-OXOACÉTICO POR DIFRAÇÃO EM PÓ DE RAIO-X E QUÍMICA QUÂNTICA

## STRUCTURAL CHARACTERIZATION OF 2-AMINO-2-OXOACETIC ACID BY X-RAY POWDER DIFFRACTION AND QUANTUM CHEMISTRY

DELGADO, Gerzon E.<sup>1\*</sup>; BELANDRIA, Lusbelly M.<sup>1</sup>, GUILLEN, Marília<sup>1</sup>, MORA, Asiloé J.<sup>1</sup>, SEIJAS, Luis E.<sup>2</sup>

<sup>1</sup> Laboratorio de Cristalografía, Departamento de Química, Facultad de Ciencias, Universidad de Los Andes, Mérida 5101, Venezuela

<sup>2</sup> Laboratorio de Procesos Dinámicos em Química, Departamento de Química, Facultad de Ciencias, Universidad de Los Andes, Mérida 5101, Venezuela

\* Correspondence author  
e-mail: gerzon@ula.ve

Received 04 July 2019; received in revised form 27 October 2019; accepted 27 October 2019

### RESUMO

O ácido 2-amino-2-oxoacético ou ácido carbamoil fórmico ou ácido oxâmico é um ingrediente farmacêutico ativo (API) de grande importância principalmente por ser um inibidor da desidrogenase láctica (LDH). Atua como um inibidor das vias metabólicas de células tumorais e exibiu atividade anticâncer significativa contra células de carcinoma nasofaríngeo (NPC) *in vitro* e pode ser considerado como uma droga potencial para o tratamento do diabetes tipo 2. Além disso, esse composto poderia ser usado como um componente no projeto de arquiteturas supramoleculares baseadas em ligações de hidrogênio através das funcionalidades complementares de ligação de hidrogênio dos grupos funcionais carbonila e amida presentes. A difração de raios X de cristal único é a técnica mais poderosa para determinar a estrutura cristalina de pequenas moléculas. No entanto, para vários materiais, incluindo o ácido oxâmico, pode ser complicado cultivar cristais únicos de tamanho e qualidade adequados que os tornem apropriados para a análise da estrutura. Por esse motivo, o estudo estrutural foi realizado com difração de raios X em pó, um processo significativamente mais desafiador do que a determinação de estruturas a partir de dados de cristal único. O ácido oxâmico foi caracterizado por técnicas espectroscópicas de FT-IR e RMN, análise térmica de TGA-DSC, cálculos semi-empíricos de PM7 e difração de raios X por pó. O composto do título cristaliza no sistema monoclínico com grupo espacial Cc, Z = 4 e parâmetros celulares unitários  $a = 9.4994(4)$  Å,  $b = 5.4380(2)$  Å,  $c = 6.8636(3)$  Å,  $\beta = 107.149(2)^\circ$ ,  $V = 338.79(2)$  Å<sup>3</sup>. A molécula tem uma conformação *trans*. A estrutura molecular e o empacotamento de cristais são estabilizados principalmente pelas ligações intra e intermoleculares de hidrogênio O - H ... O e N - H ... O. A caracterização estrutural deste tipo de composto API é importante para entender seus mecanismos de ação devido a seus consideráveis efeitos biológicos. Em particular, este estudo estrutural permitiria o exame subsequente de suas propriedades medicinais como um agente antitumoral e antidiabético.

**Palavras-chave:** ácido oxâmico, difração de raios-X, cálculo PM7, ligação de hidrogênio

### ABSTRACT

2-amino-2-oxoacetic acid, carbamoyl formic acid, or oxamic acid is an active pharmaceutical ingredient (API) of great importance mainly because is an inhibitor of lactic dehydrogenase (LDH). It acts as an inhibitor to the metabolic pathways of the tumor cells and exhibited significant anticancer activity against nasopharyngeal carcinoma (NPC) cells *in vitro* and can be considered as a potential drug for the treatment of type 2 diabetes. Also, this compound could be used as a building block in the design of supramolecular architectures based on hydrogen bonds through the complimentary hydrogen-bond functionalities of the carbonyl and amide functional groups present. Single-crystal X-ray diffraction is the most powerful technique for crystal structure determination of small molecules. However, for several materials, including oxamic acid, it could be complicated to grow single crystals of suitable size and quality that make them appropriated to structure analysis. For this reason, the structural study was conducted with powder X-ray diffraction which is a process significantly more challenging than structure determination from single-crystal data. Oxamic acid has been characterized by FT-IR and NMR spectroscopic techniques, thermal TGA-DSC analysis, semi-empirical PM7 calculations, and X-ray powder

diffraction. The title compound crystallizes in the monoclinic system with space group *Cc*, *Z*=4, and unit cell parameters *a*= 9.4994(4) Å, *b*= 5.4380(2) Å, *c*= 6.8636(3) Å, *β*= 107.149(2)°, *V*= 338.79(2) Å<sup>3</sup>. The molecule has a *trans* conformation. The molecular structure and crystal packing are stabilized mainly by intra- and inter-molecular O--H...O and N--H...O hydrogen bonds. The structural characterization of this type of API compound is important to understand its mechanisms of action due to its considerable biological effects. In particular, for oxamic acid, this structural study would allow subsequent examination of its medicinal properties as an antitumor and antidiabetic agent.

**Keywords:** oxamic acid, powder X-ray diffraction, PM7 calculation, hydrogen bonding.

## 1. INTRODUCTION

2-amino-2-oxoacetic acid, carbamoyl formic acid, or oxamic acid is an active pharmaceutical ingredient (API) of great importance mainly because is an inhibitor of lactic dehydrogenase (LDH), acts as an inhibitor to the metabolic pathways of the tumor cells (Papaconstantinou and Colowick, 1961; Zhao *et al.*, 2011; Li *et al.*, 2013) and exhibited significant anticancer activity against nasopharyngeal carcinoma (NPC) cells *in vitro* (Li *et al.*, 2013). Recently, it was demonstrated that oxamic acid improved glycemic control and insulin sensitivity in db/db mice, and therefore it can be considered as a potential drug for the treatment of type 2 diabetes (Ye *et al.*, 2016). On the other hand, oxamic acid is normally generated from the oxidation of organic compounds containing nitrogen functional groups, as aniline, sulfanilic acid and azo dyes (Leitner *et al.*, 2002), and is highly refractory to chemical oxidation and conventional processes as ozonation and photolysis (Kerna *et al.*, 2007).

From the molecular point of view (Figure 1), oxamic acid (H<sub>2</sub>NCO-COOH), the monoamide of the oxalic acid (HOOC-COOH), is the isoelectronic and isosteric analog of pyruvic acid (H<sub>3</sub>CCO-COOH), one of the most important chemical compound in biochemistry. However, the NH<sub>2</sub> group of oxamic acid makes it chemically more active, since having hydrogen donor groups (NH) and, in turn, hydrogen acceptor groups (C=O), is capable of forming interesting supramolecular arrangements in the solid-state (Aakeröy *et al.*, 1996). That is why this compound begins to be used as a building block in the design of supramolecular architectures based on hydrogen bonds through the complimentary hydrogen-bond functionalities of the carbonyl and amide functional groups (Da Cunha *et al.*, 2018). Molecules containing the oxamate group (C<sub>2</sub>O<sub>3</sub>N<sub>2</sub>-) have been synthesized during the past three decades due to their role as chelate ligands in coordination chemistry (Orge *et al.*, 2015).

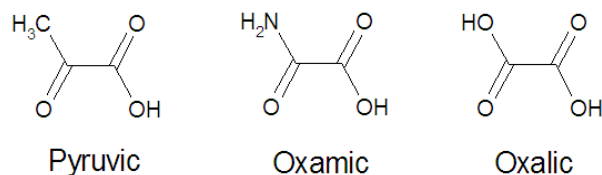


**Figure1.** Pyruvic, Oxamic and Oxalic acid chemical structures.

A search of the Cambridge Structural Database (CSD version 5.40, Nov 2018) (Groom and Allen, 2014) revealed that there are only 12 entries containing the oxamate fragment, transition-metal complexes were not included, all salts. The crystal structure of 2-amino-2-oxoacetic acid has not been reported.

Single-crystal X-ray diffraction is the most powerful technique for crystal structure determination of small molecules. However, for several materials, it could be complicated to grow single crystals of suitable size and quality that make them appropriated to structure analysis. It is difficult to recrystallize the oxamic acid reason why its structure has not been determined. Therefore, the structural study was carried out using powder X-ray diffraction, which is a process significantly more challenging than structure determination from single-crystal data (Harris and Williams, 2014).

In this work, and as part of ongoing structural studies on amino acid derivatives with active biologically molecules (Ávila *et al.*, 2004; Mora *et al.*, 2005; 2013; 2017; Seijas *et al.*, 2010; Delgado *et al.*, 2012; 2015; 2016a; 2016b; 2019; Fernández *et al.*, 2018), including the derivative nicotinamidium oxamate (Delgado *et al.*, 2015), it has been reported the spectroscopic, theoretical and powder X-ray diffraction study of 2-amino-2-oxoacetic, oxamic acid (I).

## 2. MATERIALS AND METHODS

Oxamic acid (2-amino-2-oxoacetic acid) 98% was a commercial material, purchased from Aldrich Co. (O3750), and was used as received.

Attempts to recrystallize the acid in various solvents was unsuccessful.

## 2.1 FT-IR and NMR spectroscopic studies

The FT-IR spectrum for the title compound was recorded on a Perkin Elmer 1600 spectrometer employing a KBr disc, in the region from 400 to 4000  $\text{cm}^{-1}$  (Figure 2). The bands at 3352 and 3244  $\text{cm}^{-1}$  are typical of the asymmetric tension of N-H group. The bands at 1732 and 1682  $\text{cm}^{-1}$  may be assigned to the carbonyl groups (C=O). Furthermore, the symmetric 1238  $\text{cm}^{-1}$  tension band of CO group, indicates that the oxamic acid is in neutral form.

$^1\text{H}$ -NMR and  $^{13}\text{C}$ -NMR spectra were recorded on a Bruker Avance 400 model spectrometer in DMSO- $d_6$  solution:  $^1\text{H}$  NMR (400 MHz, DMSO- $d_6$ )  $\delta$ =11.01 (s, OH),  $\delta$ =7.68 (s,  $\text{NH}_2$ ).  $^{13}\text{C}$  NMR (100.6 MHz, DMSO- $d_6$ )  $\delta$ =162.0 (C=O amide),  $\delta$ =159.8 (C=O carboxy).

## 2.2 Thermal analysis

Melting point was determined on an Electrothermal Model 9100 apparatus. Thermal analysis of oxamic acid was performed in a Perkin-Elmer TGA7 coupled with a DSC console. The sample was heated from 25 to 600  $^{\circ}\text{C}$  at a rate of 10  $^{\circ}\text{C min}^{-1}$ , under a nitrogen flux of 100  $\text{ml min}^{-1}$  (Figure 3). A sharp endothermic peak observed at 206  $^{\circ}\text{C}$  corresponds to the compound melts, which was further confirmed by melting point analysis (205-206  $^{\circ}\text{C}$ ). The sample decomposed completely at 290  $^{\circ}\text{C}$ .

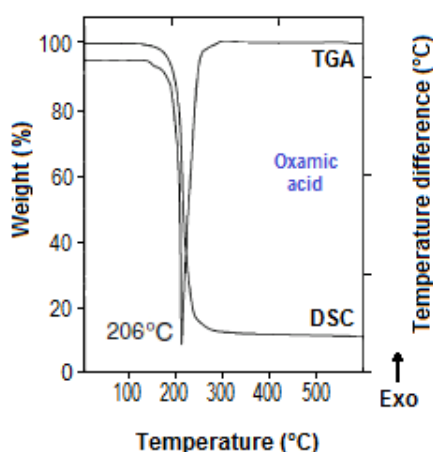


**Figure 3.** Thermal analysis plot, TGA and DSC, for (I).

## 2.3 Theoretical calculations

In order to complete and improve the

initial model for further Rietveld refinement (Rietveld, 1969), it was decided to perform a geometry optimization of the solid, employing the semi-empirical quantum mechanics method PM7 (Stewart, 2013). In addition, the reported average unsigned errors for bond length in organic compounds containing C, H, N, O are around 0.01 Å. The initial lattice parameters for the crystal was obtained from the X-ray diffraction pattern indexing and the non-hydrogen atomic positions were obtained from the crystal structural solution found by direct methods using the program Expo2009 (Altomare *et al.*, 2009) in the Cc monoclinic space group. From the Direct Methods solution, we are not able to assign the N and O atoms of the molecules, and it was decided to perform an optimization geometry considering four conformers (Figure 4), and hydrogen atoms were placed depending on the atom assignments. All the calculations were performed using Gaussian09 (Frisch *et al.*, 2009); the lattice parameters were fixed to the experimental values and the atomic positions were optimized.

For all the calculations the basis set 6-31++G(d,p) was employed. The initial structure was built up using bond distances and angles of crystal structure reported in this work. To visualize non-covalent interactions Non-Covalent-Index (NCI) based on the analysis of the electron density was used (Johnson *et al.*, 2010). This approach has the ability to highlight interactions on the low density, low gradient regime. NCI analysis allows us to identify different types of chemical interactions in terms of the electron density and its gradient.

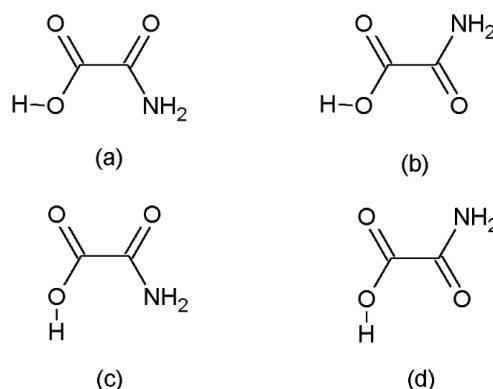


**Figure 4.** Conformers, cis and trans, considered for the geometrical optimization of (I).

The NCI analysis is based on a 2D plot of the reduced gradient density (RGD) vs the electron density ( $\rho$ ) where:  $\text{RGD} = 1/2(3\pi^2)^{1/3} \cdot |\nabla\rho|/\rho^{4/3}$ . When inter or intramolecular interaction is present, the RGD goes to zero as a result of the presence of critical points in the

electron density between the interacting fragments.

## 2.4. X-ray powder diffraction

The X-ray powder diffraction pattern for 2-amino-2-oxoacetic acid was collected at room temperature in a Siemens D5005 diffractometer using monochromatized CuK $\alpha$  radiation. A small quantity of the sample was ground mechanically in an agate mortar and pestle and mounted on a flat holder covered with a thin layer of grease. The samples were scanned from 15–65° 2 $\theta$ , with a step size of 0.02° and counting time of 10s. Silicon was used as an external standard.

From the powder pattern, the 20 first measured reflections were completely indexed using the program Dicvol04 (Boultif and L  uer, 2004), which gave a unique solution in a monoclinic cell with parameters  $a = 9.50 \text{ \AA}$ ,  $b = 5.44 \text{ \AA}$ ,  $c = 6.86 \text{ \AA}$ ,  $\beta = 107.1^\circ$  in a C-type cell. The Rietveld refinement (Rietveld, 1969) was carried out using the Fullprof program (Rodr  guez-Carvajal, 2018) with the unit cell parameters indexed and the atomic positions theoretically optimized. The angular dependence of the peak full width at half maximum (FWHM) was described by the Cagliotti's formula (Cagliotti *et al.*, 1958). Peak shapes were described by the parameterized Thompson-Cox-Hastings pseudo-Voigt profile function (Thompson *et al.*, 1987). The background variation was described by a polynomial with six coefficients. Restraints were applied to bond distances (deviations  $\pm 0.01 \text{ \AA}$ ) and bond angles (deviations  $\pm 1^\circ$ ) using average values derived from the CSD [10]. The isotropic atomic displacement parameters were refined as one overall Uiso for the non-hydrogen atoms starting from a value of  $0.03 \text{ \AA}^2$ . The isotropic displacement coefficients of each of the hydrogen atoms were calculated as 1.3 times the value of the temperature factor of their riding non-hydrogen atom. The refinement was stable and convergence was readily achieved. All geometrical calculations were done using the program Platon (Spek, 2003). Table 1 summarizes the crystal data, intensity data collection and Rietveld refinement details for the title compound. Figure 5 shows the observed calculated and different profile for the final cycle of the refinement. Table 2 shows the atomic coordinates and selected geometrical parameters for 2-amino-2-oxoacetic acid.

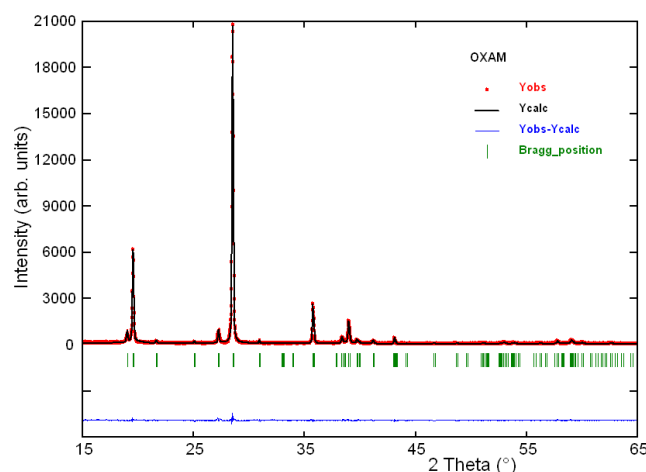


Figure 5. Rietveld refinement plot for (I).

CCDC-1500810 contains the supplementary crystallographic data for this paper. These data can be obtained free of charge from the Cambridge Crystallographic Data Centre via [www.ccdc.cam.ac.uk/data\\_request/cif](http://www.ccdc.cam.ac.uk/data_request/cif).

## 3. RESULTS AND DISCUSSION:

The 2-amino-2-oxoacetic acid crystallizes in the non-centrosymmetric space group Cc with one molecule in the asymmetric unit. Figure 6 shows the molecular structure and the atom-labeling scheme of the title compound. Bond distances, bond angles, and torsion angles are presented in Table 2, and are in agreement with experimental average values found in the 12 entries with oxamate fragments, searched in the Cambridge Structural Database (CSD, version 5.40, Nov 2018) (Groom and Allen, 2014).

This compound crystallizes in a neutral form, unlike the oxamate fragments found in the crystal structural database. The neutral character of the amino acid is confirmed by a clear difference in the values for C1–O1 and C1–O2 bond distances (Table 2). The molecule is essentially plane with maximal deviations of 0.001(1)  $\text{\AA}$  in C1, and adopts a *trans* conformation with the acid and amide groups on opposite sides of the molecule [torsion O1–C1–C2–N2 = 178.6(2)  $^\circ$ ].



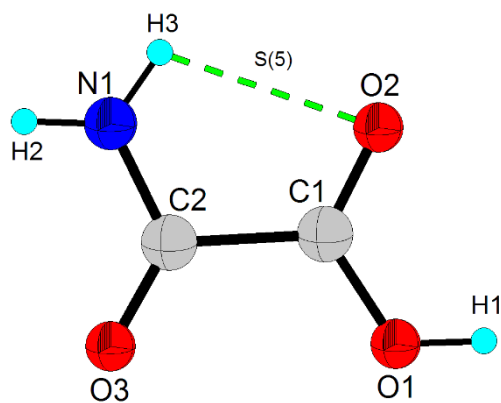


**Figure 6.** The molecular structure of (*I*) showing the atomic numbering scheme.

The molecular structure and crystal packing are stabilized by one intermolecular O–H...O and three N–H...O hydrogen bonds, reinforced by one N–H...O intramolecular interaction (Table 3). The intramolecular N1–H3...O2 gives rigidity to the oxamate molecule with graph-set motif S(5) (Etter, 1990). The intramolecular interactions O1–H1...O3 and N3–H3...O2 produces a hydrogen bond that connect two molecules by a typical heterosinton amide-acid with graph-set  $R^2_2(8)$ . The N1–H3...O3 hydrogen bonds form infinite chains which run along the *c* axis with graph-set notation C(4) and produce another heterosinton  $R^2_2(8)$  with the N1–H2...O2 interaction. Together, these hydrogen-bond patterns produce a 14-atom cycle described by  $R^3_4(14)$ , which are connected by amide-acid  $R^2_2(8)$  dimers (Figure 7). These chains which extend along the *c* and *b* axis resulting in a lamellar packing type with layers of chains stack along the diagonal of *ca* plane with an average interplanar separation of 5.18 Å (Figure 8).

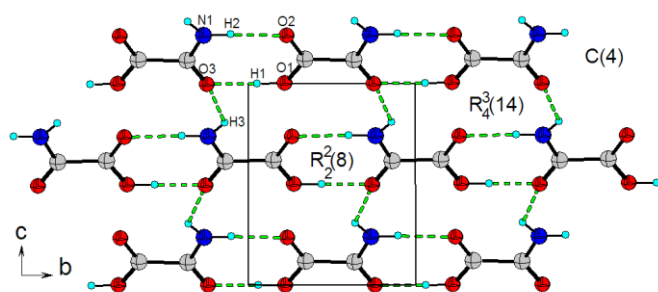


**Figure 7.** A portion of the crystal packing shows all intermolecular N–H...O and O–H...O intramolecular hydrogen bonds formed in (*I*).

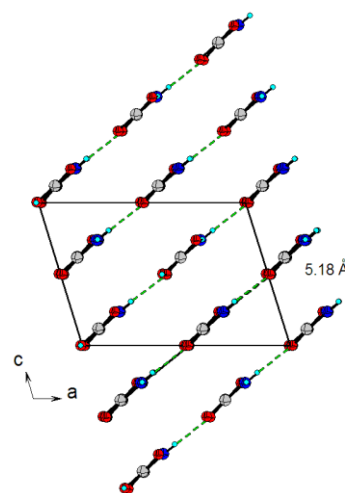


**Figure 8.** Packing view of (*I*) showing the extended chains in the *ca* plane and separated 5.18 Å along the diagonal.

Figure 9 shows a graph of RGD vs  $\text{sing}(\lambda_2)\rho$ , where each of the points has been colored with the corresponding value of  $\text{sing}(\lambda_2)\rho$ . As mentioned above, the peaks in the graph are coupled with non-covalent interactions and the value of the density where RGD tends to zero is associated with the strength of the interaction, the negative sign indicates whether the interaction is attractive, while the positive sign indicates repulsive interactions. The hydrogen bonds interactions are in agree the experimental results and the NCI analysis of the non-covalent interactions indicates that the force of the hydrogen bonds decreases in the following order: O1–H1...O3 (i) > N1–H2...O2 (ii) > N1–H3...O3 (iii) > N1–H3...O2.

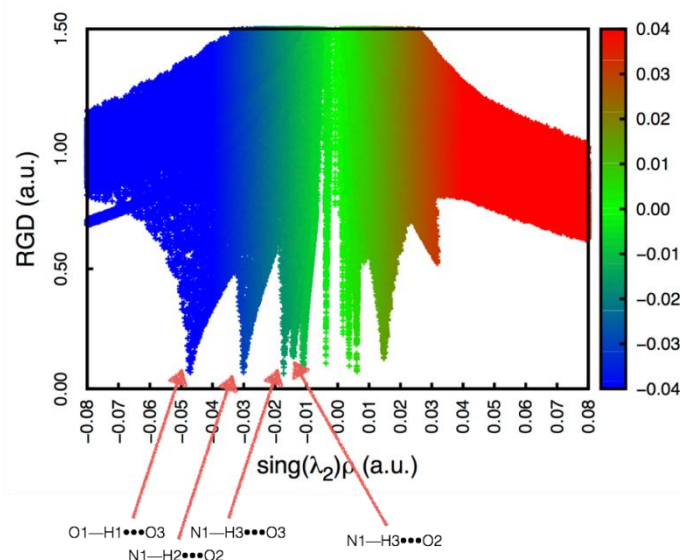


**Figure 9.** RGD diagram shows the hydrogen bond interactions in agree with the experimental results in (*I*).

#### 4. CONCLUSIONS:

2-amino-2-oxoactic acid, oxamic acid, an active pharmaceutical ingredient (API) of great importance mainly as possible anti-tumor and anti-diabetes agent, has been structurally characterized by theoretical and experimental techniques. The impossibility of obtaining adequate crystal for single-crystal diffraction study made it necessary to use powder X-ray diffraction complemented by PM7 calculations to establish its crystal structure.

Oxamic acid crystallizes in the monoclinic system with space group *Cc*, *Z*=4, and unit cell parameters *a*= 9.4994(4) Å, *b*= 5.4380(2) Å, *c*= 6.8636(3) Å,  $\beta$ = 107.149(2)°, *V*= 338.79(2) Å<sup>3</sup>. The bond lengths and bond angles are very close to the corresponding ones found in Cambridge structural database. The molecule has a *trans* conformation. The molecular structure and crystal packing are stabilized mainly by intra- and inter-molecular O--H...O and N--H...O hydrogen bonds.

The structural characterization of oxamic acid can contribute to the chemical and pharmaceutical industries because of its potential use as antitumor and antidiabetic agent.

#### 5. ACKNOWLEDGMENTS:

This work was supported by CDCHT-ULA (Grant C-1990-17-08-B) and FONACIT (Grants LAB-97000821).

#### 6. REFERENCES:

1. Papaconstantinou, J., Colowick, S.P. *J. Biol. Chem.* **1961**, 236, 278.
2. Zhao, Y., Liu, H., Liu, Z., Din, Y., LeDoux, S.P., Wilson, G.L., Voellmy, R., Lin, Y., Lin, W., Nahta, R., Liu, B., Fodstad, O., Chen, J., Wu, Y., Price, J.E., Tan, M. *Cancer Res.* **2011**, 71, 4585.
3. Li, X., Lu, W., Hu, Y., We, S., Qian, C., Wu, W., Huang, P. *Int. J. Oncol.*, **2013**, 43, 1710.
4. Ye, W., Zheng, Y., Zhang, S. Yan, L., Cheng, H., Wu, M. *Plos One*, **2016**, 11, e,0150303
5. Leitner, N.K.V., Berger, P., Legube, B. *Environ. Sci. Technol.* **2002**, 36, 3083.
6. Kerna, A., Tilleyblain, E., Hunter, S. *J. Biotechnol.*, **2007**, 29, 6.
7. Aakeröy, C., Hughes, D., Nieuwenhuyzen, M. *J. Am. Chem. Soc.*, **1996**, 118, 10134.
8. Da Cunha, T.T., Oliveira, W.X.C., Marzano, I.M., Pinheiro, C.B., Pereira-Maia, E.C., Pereira, C.L.M. *J. Mol. Struct.* **2018**, 1149, 803.
9. Orge, C.A., Pereira, M.F., Faria, J.L. *Appl. Catal. B*, **2015**, 174-175, 113.
10. Groom, C.R., Allen, F.H. *Angew. Chem. Int. Ed.*, **2014**, 53, 662.
11. Harris, K.D.M., Williams, P.A. in *Structure from Diffraction Methods*, ed. by D.W. Bruce, D. O'Hare, R.I. Walton, Wiley, Chichester, **2014**.
12. Ávila, E.E., Mora, A.J., Delgado, G.E., Ramírez, B., Bashas, A., Koteich, S. *Acta Cryst. C*, **2004**, 60, o759.
13. Mora, A.J., Ávila, E.E., Delgado, G.E., Fitch, A.N., Brunelli, M. *Acta Cryst. B*, **2005**, 61, 96.
14. Seijas, L.E., Delgado, G.E., Mora, A.J., Brunelli, M., Fitch, A.N. *Powder Diffraction*, **2010**, 25, 235.
15. Delgado, G.E., Seijas, L.E., Mora, A.J., Gonzalez, T., Briceño, A. *J. Chem. Cryst.* **2012**, 42, 968.
16. Mora, A.J., Belandria, L.M., Ávila, E.E., Seijas, L.E., Delgado, G.E., Miró, A., Almeida, R., Brunelli, M., Fitch, A.N. *Cryst. Growth Design*, **2013**, 13, 1849.
17. Delgado, G.E., Varela, K.N., Mora, A.J., Bruno, J., Atencio, R. *Mol. Cryst. Liq. Cryst.* **2015**, 609, 218.
18. Delgado, G.E., Mora, A.J., González, T., Uzcátegui, J., Lobaton, R., Marroquín, G. *Mol. Cryst. Liq. Cryst.* **2016a**, 625, 225.
19. Delgado, G.E., Guillén, M., Ramírez, J.W., Mora, A.J., Contreras, J.E., Chacón, C. *Powder Diffraction*, **2016b**, 31, 242.
20. Mora, A.J., Belandria, L.M., Delgado, G.E., Seijas, L.E., Lunar, A., Almeida, R. *Acta Cryst. B*, **2017**, 73, 968.
21. Fernández, L.E., Delgado, G.E., Maturano, Tótar, R.M., Varetti, E.L. *J. Mol. Struct.* **2018**, 1168, 84.
22. Delgado, G.E., Mora, A.J., González, T., Santos, I., Rivas, P., Seijas, L.E. *J. Tchê Quím.* **2019**, 16, 875.
23. Rietveld, H.M. *J. App. Cryst.* **1969**, 2, 65.

24. Stewart, J.J. *J. Mol. Model.*, **2013**, 19, 1.
25. Altomare, A., Camalli, M., Cuocci, C., Moliterni, A., Rizzi, R., Corriero, N., Falcicchio, A. *J. Appl. Cryst.* **2009**, 42, 1197.
26. Frisch, M.J. *et al.* Gaussian 09, Gaussian, Inc., **2009**.
27. Jhonson E. R., Keinan S., Mori-Sánchez P., Contreras-García, J., Cohen A.J., Yang, W. *J. Am. Chem. Soc.* **2010**, 132, 6498.
28. Boulton, A., Löser, D. *J. Appl. Cryst.* **2004**, 37, 724.
29. Rodriguez-Carvajal J. Fullprof, version 6.2, **2018**, LLB, CEA-CNRS, France.
30. Cagliotti, G., Paoletti, A., Ricci, F.P. *Nucl. Instrum.* **1958**, 3, 223.
31. Thompson, P., Cox, D.E., Hastings, J.B. *J. App. Cryst.* **1987**, 20, 79.
32. Spek, A.L. *J. Appl. Cryst.* **2003**, 36, 7.
33. Etter, M.C. *Acc. Chem. Res.* **1990**, 23, 120.

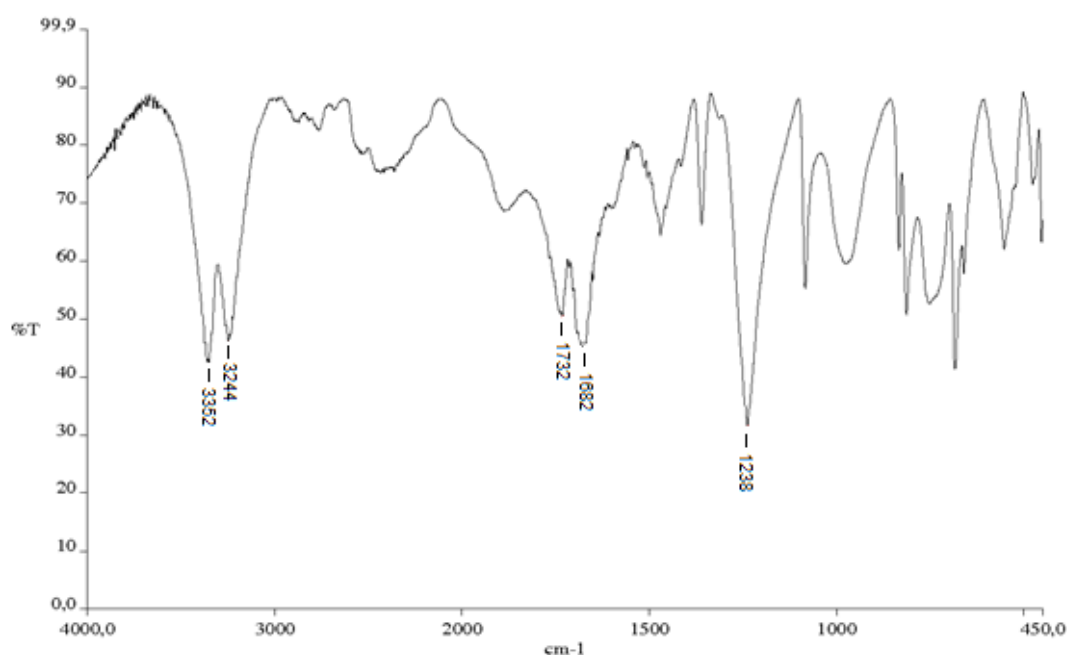


**Figure 2.** FT-IR spectrum for (I).

**Table 1.** Results of the Rietveld refinement for oxamic acid (I).

Molecular formula	C <sub>2</sub> H <sub>3</sub> NO <sub>3</sub>	CCDC	1500810
Molecular weight	89.05 (g/mol)		
Crystal system	Monoclinic	D <sub>calc</sub>	1.752 (g/cm <sup>3</sup> )
Space group	Cc (N° 9)	N° step intensities	2501
Z	4	N° independent reflections	153
a	9.4994(4) Å	Peak-shape profile	Pseudo-Voigt
b	5.4380(2) Å	R <sub>exp</sub>	5.2 %
c	6.8636(3) Å	R <sub>p</sub>	7.7 %
β	107.149(2)°	R <sub>wp</sub>	7.2 %
V	338.79(2) Å <sup>3</sup>	S	1.4

$$R_{\text{exp}} = 100 \left[ \frac{(N-P+C)}{\sum w(y_{\text{obs}})^2} \right]^{1/2}$$

$$R_p = 100 \frac{\sum |y_{\text{obs}} - y_{\text{calc}}|}{\sum |y_{\text{obs}}|}$$

$$R_{\text{wp}} = 100 \left[ \frac{\sum w |y_{\text{obs}} - y_{\text{calc}}|^2}{\sum w |y_{\text{obs}}|^2} \right]^{1/2}$$

$$S = [R_{\text{wp}} / R_{\text{exp}}]$$

N-P+C: number of degrees of freedom

**Table 2.** Atomic coordinates and geometrical parameters ( $\text{\AA}$ , deg) for oxamic acid (**I**).

Atom	x	y	z	foc	B ( $\text{\AA}^2$ )
C1	0.1069(2)	1.1538(2)	-0.3812(2)	1	0.15(3)
C2	0.1067(2)	0.8628(2)	-0.3851(2)	1	0.15(3)
O1	-0.0056(2)	1.2762(2)	-0.4988(2)	1	0.15(3)
O2	0.2078(2)	1.2632(2)	-0.2635(2)	1	0.15(3)
O3	0.0108(2)	0.7437(2)	-0.5023(2)	1	0.15(3)
N1	0.2299(2)	0.7632(2)	-0.2609(2)	1	0.15(3)
H1	-0.0059(2)	1.4402(2)	-0.5006(2)	1	0.45(4)
H2	0.2372(2)	0.6025(2)	-0.2572(2)	1	0.45(3)
H3	0.3008(2)	0.8578(2)	-0.1929(2)	1	0.45(3)
C1-O1	1.313(2)		C2-O3	1.209(2)	
C1-O2	1.210(2)		C2-N1	1.341(2)	
C1-C2	1.582(2)		N1-C2-C1	113.4(1)	
O1-C1-C2	120.0(1)		O2-C1-C2	119.9(2)	
O3-C2-C1	122.9(1)		O1-C1-O2	120.0(1)	
O1-C1-C2-N1	178.6(2)		O1-C1-C2-O3	4.9(3)	
O2-C1-C2-O3	-178.3(2)		O2-C1-C2-N1	-4.6(2)	

**Table 3.** Hydrogen bonds geometry ( $\text{\AA}$ , deg) (*D*-donor; *A*-acceptor; *H*-hydrogen) for (**I**).

D--H...A	D--H	H...A	D...A	D--H...A
N1--H3...O2 (intra)	1.030	2.310	2.697(7)	101.00
O1--H1...O3 <sup>(i)</sup>	1.030	1.670	2.694(7)	176.00
N1--H2...O2 <sup>(ii)</sup>	1.030	1.720	2.744(7)	169.00
N1--H3...O3 <sup>(iii)</sup>	1.030	2.040	3.049(4)	168.00
N1--H2...O1 <sup>(iii)</sup>	1.030	2.600	2.993(4)	102.00
Symmetry codes: <sup>(i)</sup> x, 1+y, z, <sup>(ii)</sup> x, -1+y, z, <sup>(iii)</sup> 1/2+x, -1/2-y, 1/2+z				